

UNIVERSITY OF
Waterloo



Department of Mechanical and Mechatronics Engineering

CMD

A Report Prepared For:
The University of Waterloo,
MTE 482: Mechatronics Engineering Design Workshop Teaching Team

Prepared by Group 27:
Abhi Gupta, 20757207
Avinash Reddy Yarram, 20827096
Arshak Petrosyan, 20766444
Mohamed Moustafa, 20790387
Nigel Fernandes, 20827918

April 8, 2024

April 8, 2024

Prof. Andrew Kennings
Department of Electrical and Computer Engineering
Prof. Behrad Khamesee
Department of Mechanical and Mechatronics Engineering
University of Waterloo
200 University Ave W.
Waterloo, Ontario, N2L 3G1

Dear Professors Kennings and Khamesee,

We are writing to formally submit our final design report for the MTE 482 capstone project. This report for our project "CMD" was completed by a team of the following 4B Mechatronics Engineering students: Abhi Gupta, Arshak Petrosyan, Avinash Reddy Yarram, Mohamed Moustafa, and Nigel Fernandes.

This report represents the culmination of the work on "CMD", from conception through to the completion and presentation at the symposium day. It covers the rigorous process we underwent in achieving the final design, detailing the modifications and deviations from the original plan, the construction and manufacturing process, finding sponsors, as well as the testing and performance evaluation of our project.

The project's compliance with the required standards and safety guidelines, as well as a comprehensive overview of the journey from previous designs to the final design and its realization, are covered in this report. This report also contains detailed information about criteria, objectives, constraints, budget, scheduling, and more. The report is still accurate, current, and relevant to the completed project as of the date of this letter.

This report was written entirely by the undersigned team members and has not been submitted for academic credit elsewhere. We have all thoroughly reviewed the content of this report and endorse its findings and conclusions.

Best Regards,


Abhi Gupta,



Avinash Reddy Yarram,



Arshak Petrosyan,



Mohamed Moustafa,



Nigel Fernandes



Table of Contents

List of Figures	iii
List of Tables	v
Executive Summary	vi
1.0 Introduction / Background.....	1
2.0 Problem Definition/Formulation	1
2.1 Needs Analysis/Project Stakeholders	1
2.2 Problem Formulation	1
2.3 Constraints	2
2.4 Criteria.....	2
3.0 Summary of Initial Design	2
3.1 Track Design	2
3.2 Wheel and Tire Selection.....	3
3.3 Motor Selection.....	3
3.4 Chain Drive Mechanism.....	3
3.5 Brakes	3
3.6 Suspension.....	4
3.7 Self-balancing.....	4
3.8 Stair Climbing	4
3.9 Chassis	5
3.10 Electronics.....	5
3.11 Software and control.....	5
4.0 Final Design	6
4.1 Final Design/Modifications from the Original Design	6
4.1.1 Track System	6
4.1.2 Angling Mechanism.....	6
4.1.3 Turning System	8
4.1.4 Chassis	8
4.1.5 Electrical System.....	10
4.1.6 Code Architecture	13
4.2 Construction/Manufacturing	14
4.2.1 Track System	15

4.2.2 Chassis	15
4.2.3 Turning System	17
4.2.4 Electrical System.....	18
4.3 Commissioning.....	19
4.3.1 Motor Control Testing.....	19
4.3.2 Linear Actuator Control Testing.....	20
4.3.3 IMU Feedback.....	21
4.4 Testing and Performance	21
4.4.1 Durability Test.....	21
4.4.2 User comfort and safety.....	21
4.4.3 Control system	21
5.0 Scheduling and Budget.....	21
5.1 Schedule	21
5.2 Original Expected Budget.....	22
5.3 Actual Spent Budget.....	23
6.0 Conclusions and Recommendations	24
7.0 Teamwork	25
7.1 Teamwork Efficiency/Breakdown.....	25
7.2 Task Completion of Each Member.....	25
References	26
Appendix A: Detailed Information and Calculations.....	27
Appendix B: Bill of Materials and Part References	34
Appendix C: As Built Drawings.....	38
Appendix D: Device Code	41

List of Figures

Figure 1: a) original two track system [3] b) mono-track system used.	6
Figure 2: Initial Hydraulic orientation.	7
Figure 3: Angling Mechanism.....	7
Figure 4: Chain connection to chassis.....	8
Figure 5: Initial Chassis Track Configuration	9
Figure 6: New Chassis Track Configuration	9
Figure 7: Motor Mounts	9
Figure 8: Complete Chassis.....	10
Figure 9: Arduino Mega 2560 Board [5].....	11
Figure 10: LM317 Adjustable Voltage Regulator Pinout and Resistor Diagrams [6]	12
Figure 11: PA-17-8-2000-POT Actuator [7] and BTS 7960 Dual H-Bridge motor controller [8] ..	12
Figure 12: Labelled Joysticks Controls.....	14
Figure 13: integrated suspension system and drive gear.	15
Figure 14: Step 1 Assembly	16
Figure 15: Step 2 Assembly	16
Figure 16: Step 3 Assembly	16
Figure 17: Step 4 Assembly	17
Figure 18: Step 5 Assembly	17
Figure 19: Full Electrical Schematic of the CMD	18
Figure 20: PA-17 linear actuator, Arduino, and BTS7960 pinout diagram [8].....	20
Figure 21: CMD Project Timeline in 2024.....	22
Figure 22: Initial Track Design.....	27
Figure 23: Initial Powertrain System.....	27
Figure 24: Worst Case Free Body Diagram.....	28
Figure 25: Angling Mechanism Reference Frame	29
Figure 26: Chassis Free Body Diagram	30
Figure 27: Initial Chassis Measurements.....	31
Figure 28: Support Member Angles.....	32
Figure 29: Summary of All the dimensions	33
Figure 30: CIM motor [10]	35
Figure 31: Talon SRX Motor Controller [4]	35
Figure 32: Fuses for all components	35
Figure 33: Emergency Disconnect front and back.....	36
Figure 34: Full CMD electrical assembly.	36
Figure 35: Initial Chassis Structure.....	36
Figure 36: FEA results of stresses.	37
Figure 37: Complete CAD of the wheelchair.	37
Figure 38: New Design Fully Assembled.....	37
Figure 39: Piece 1 Drawing.....	38
Figure 40: Piece 3 Drawing.....	38
Figure 41: Piece 5 Drawing.....	39
Figure 42: Piece 7 Drawing.....	39

Figure 43: Piece 8 Drawing	39
Figure 44: Piece 9 Drawing	40
Figure 45: Piece 10 Drawing	40
Figure 46: CIM Motor manufacturer specification sheet and component drawing [10].....	40

List of Tables

- Table 1: Selection Criteria for Competing Designs [1] 2
- Table 2: Fuses Used 13
- Table 3: Budget for materials [1] 23
- Table 4: Final Amount Spent 24
- Table 5: Chosen Electronics 33
- Table 6: Chassis Bill of Materials 34
- Table 7: Electronics Bill of Materials 34

Executive Summary

A need was identified in populations with limited to no use of their legs for a mobility device that would allow them to traverse all terrain while specifically targeting uneven surfaces, small staircases, single steps, and snow. While modified wheelchair solutions exist on the market today, they either fail to meet these needs effectively or are sold at an unreasonable price point. CMD set out to give these populations the mobility they desperately need at a reasonable cost by creating a wheelchair attachment, taking large inspiration from the modern snowmobile.

The device made use of a snowmobile track as its primary drive system, desirable for its high traction and aptitude for winter conditions. Castor wheels were added to the front of the device to enable steering, replacing the skis typically found on a snowmobile. Motors were selected to provide the necessary torque to propel the device and navigate obstacles in combination with a planetary gearbox system. The integrated suspension system in the snowmobile track ensured that the rider remained comfortable while traversing rough terrain by absorbing impact. An electric cylinder was used to keep the rider balanced and prevent them from tipping, particularly during stair climbing.

The chassis was constructed from square aluminum tubing as a strong but lightweight solution, with extensive force and motion analysis performed to ensure effective design and structural integrity. Necessary acceleration and incline information was collected using sensors mounted onto the device. The sensors were connected to a microcontroller with sufficient current supply and GPIO ports to accommodate them, and a battery was selected in turn to power the microcontroller and sensors, as well as the motors and electric cylinder. Software for the device was developed to allow the user to easily control the device with two analog sticks, freeing their hands to pilot the intuitive steering mechanism, as well as to ensure the user remained safe and balanced during stair climbing using sensor feedback.

This attachment to the conventional wheelchair allows users to navigate rough terrain, small bumps, and staircases while enduring winter weather conditions and ensuring the user is safe and comfortable during a full day of operation on a single charge without ever leaving their wheelchair. The device can be thought to function similarly to a bike, being embarked and disembarked as needed to traverse outdoor obstacles. The solution avoids the consumer having to buy a new wheelchair, minimizes size and mass, and allows a device tailored to outdoor use.

1.0 Introduction / Background

Wheelchair users face difficulty while attempting to navigate the world. They sometimes have to meticulously plan routes to be able to get to certain places and sometimes it is just not possible for them to access some locations if ideal conditions are not present. A prime example of this is the University of Waterloo campus, where many old buildings were not designed with accessibility in mind. Certain areas of campus, like the entrances to MC, are inaccessible if the person is using a conventional wheelchair. Some other areas might require a time-consuming, roundabout route for wheelchair users. SCH is an example of that since it is only accessible from the ring road entrance. The accessibility issues are made worse by ledges and small bumps like the ION tracks, steep or slippery inclines used by some ramps intended as an accessibility feature, unpaved or unmaintained surfaces such as parking lots which cover large portions of campus, and harsh winter conditions. Most available solutions do not adequately address these accessibility challenges, and those that do are unreasonably expensive [1].

2.0 Problem Definition/Formulation

Based on the issues outlined above, stakeholders were contacted to clarify their requirements, formulate a precise problem statement, and establish specific goals, constraints, and criteria [1].

2.1 Needs Analysis/Project Stakeholders

Two stakeholders were contacted to gain a better understanding of the issues that wheelchair users face daily. In both cases, stairs presented the biggest issue since a lot of buildings have stairs in front of their entrance. Allowing individuals to climb and descend outdoor stairs would save wheelchair users a substantial amount of time as they would be able to access more buildings without needing to change their route and look for alternate entrances. The stakeholders also mentioned other issues like wheel traction on inclines, battery life, winter weather operation, and small bumps/ledges [1].

2.2 Problem Formulation

Based on the issues described by the stakeholders, the project aimed to address both short and long-term needs for people with limited to no use of their legs. The goal was to create a mobility device that would allow users to traverse everyday obstacles such as stairs, small bumps, and unpaved surfaces. The device must function effectively in typical commuting conditions which include snow, rain, inclined surfaces, and small obstacles. Furthermore, the user must feel safe and secure during the operation of the device, and a full day's use must be achievable on a single full charge [1].

2.3 Constraints

The essential constraints of the device govern its mass, size, and safety. The device must weigh a maximum of 70kg and must not exceed a size of 56" length, 36" width, and 32" height. This will ensure that the device will be reasonable to store in cars and airplanes based on the CR9 spec [2]. To keep the user safe, the device must possess a safety kill switch, and some form of seatbelt or harness [1].

2.4 Criteria

To effectively test and assess wheelchair design during the building phase, it is essential to organize and summarize all objectives and constraints along with their corresponding metrics, criteria, and units into a comprehensive table as shown in Table 1. This structured methodology not only streamlines the assessment process but also ensures that the device adheres to the desired specifications, optimizing its functionality and user experience [1].

Table 1: Selection Criteria for Competing Designs [1]

Objective/Constraint	Basis for Measurement	Criteria	Units
Travel Safe (mass)	Mass of the device	Mass	kg
Travel Safe (size)	Linear dimensions	Size	in
Safety	Vote from each member	Safety	Yes/No
Obstacle Navigation	Vote from each member	Scale	1-10
Operation Time	Range traveled	Distance	km
Inexpensive	Manufacturing cost	Cost	\$ CAD
Aesthetic	Vote from each member	Scale	1-10

3.0 Summary of Initial Design

3.1 Track Design

The primary mechanism for enabling stair climbing revolves around the treads, with the tread design being heavily influenced by what is available in the market. The best option on the market for the tracks was a set from Super Droid Robots. The most optimal track that was available was a 4" width tread with an 85" internal circumference. The corresponding drive gear set that mated with the treads was a 1.89" pitch with an 8.9" outer diameter [1].

3.2 Wheel and Tire Selection

The Selection of wheels was guided by three main criteria: compatibility with device's dimensions, device's resistance to weather condition, and ease of acquisition. 700c wheels were chosen, a common bicycle size with a diameter of approximately 70cm. The Michelin Stargrip is a non-studded winter bicycle tire built for the 700c wheels. This tire was selected as it provided good traction in snow while also being suitable for indoor settings [1].

3.3 Motor Selection

The motor and gear ratios were selected based on the worst-case scenario torque requirement and the desired top speed for normal drive. The maximum stair angle is forty-five-degree incline staircase and weights of 70kg for the device and 120kg for the rider were considered. The ElectroCraft MP36 32:1 motor possesses 110Nm of torque and would be paired with a 6:1 ratio sprocket to achieve 660Nm of torque. For top speed calculations, the MP36's no-load speed of 115rpm was used with the 0.35m radius of the 700c wheel and a 1:1 gear ratio was assumed to start. For top speed calculations, the MP36's no-load speed of 115rpm was used with the 0.35m radius of the 700c wheel and a 1:1 gear ratio was assumed to start [1].

3.4 Chain Drive Mechanism

Sprocket selection was performed using the gear ratios. The pairing of a 6280K41 sprocket on the motor shaft with and a 6280K811 sprocket on the wheel shaft would be used to satisfy the 2:1 gear ratio for the drive wheels, and a 6280K42 sprocket on the motor shaft with a 6236K377 sprocket would be used to satisfy the 6:1 gear ratio for the treads. The motor connects to a 5/4" shaft with a threaded hole, allowing it to interface with the motor output shaft with 0.984" diameter. The shaft would be stepped to 5/8" and then to 1/2" to accommodate the two sprockets and constrain them, while the wheel and tread shafts would be stepped from 1" to 5/8" diameter to fit their respective sprockets. All the sprockets are designed for an ANSI 40 roller chain with a 1/2" pitch such as the Tsubaki 1/2" pitch ANSI roller chain, which will be used to connect both sets. As well, three bearings were used to fully define the shafts and support the radial loads they experience. The 6280K41 sprocket was paired with the 60355K691 roller bearing, and both the 6236K77 and 6280K811 sprockets were paired with 60355K733 roller bearings. Shielded bearings were used to aid in weatherproofing the device [1]. Detailed figures can be seen in Appendix A: Detailed Information and Calculations.

3.5 Brakes

Motor braking systems are unique in their reliance on electronic control, which affords them excellent precision. Though motor braking is good, loss of power to the battery or motor failure can be dangerous and risk the user's safety. Therefore, it is important to have an additional braking system such as friction braking implemented through a toggle brake design. This acts as an emergency brake giving the user more control in unexpected situations and difficult terrain [1].

A toggle brake system is analyzed for a wheelchair, featuring a mechanical advantage of 2, based on an effort arm of 0.1 cm and a load arm of 0.05 cm. This system requires a user-applied force that generates 800.4N due to friction, resulting in a braking torque of 24 Nm. To engage the brake, a force of 160 N is needed on the brake lever, considering a brake lever length of 0.15 meters and a safety factor of 1.5 for reliability. The actual pivot force is calculated to be 240N [1].

3.6 Suspension

For selecting an appropriate coil over damper suspension system, the considerations include the vehicle's total weight, the distribution of this weight across the wheels, and the desired level of ride comfort. Given a total weight of 500lbs distributed evenly between two wheels, each wheel bears 250lbs. Aiming for a comfortable ride entails a compression target of 25mm in the suspension system. Consequently, this setup necessitates a spring constant of 45.36N/mm for effective weight support and shock absorption, alongside a damping constant of at least 1450.78Ns/m to manage the rate of energy dissipation and ensure the desired ride quality [1].

3.7 Self-balancing

The self-balancing mechanism is designed to ensure a stable seating posture for the user across various staircase angles. It employs a combination of sensors and actuators to dynamically regulate the orientation of the seat, making adjustments in real time to counteract any shifts in angle, thereby maintaining balance. A 2-cylinder electric actuator is selected due to the system's smoothness and quick response. It stands out for its efficiency, demonstrating the most effective use of power and ensuring tasks such as stair climbing are performed with minimal energy expenditure. At least 106.04N of force needs to be supplied by each actuator to push the total weight of 300lbs. Using a factor of 2, a specific linear actuator from Progressive Automation with a part number of PA-09 has been selected. The selected actuator has a fully extended length of 41.71inch (1.06m) including the cylinder and static and dynamic forces of 330lbs each. Therefore, each of the 2 cylinders have a maximum capacity of producing 330lbs of force which satisfies the requirement and has a safety factor of 2.2 [1].

3.8 Stair Climbing

The stair climbing mechanism is the heart of our wheelchair innovation, enabling users to ascend and descend stairs with ease and safety. The core of the stair climbing mechanism consists of two pairs of motorized tracks on either side of the wheelchair. These tracks are equipped with high traction rubber belts that provide a good grip to go up the staircase. As the wheelchair approaches a staircase for ascent, the design ensures the tracks engage with the first step effortlessly, thanks to their grip and height exceeding the typical step height. A gyroscope sensor, mounted on the track's chassis, detects any angular shift. In response, electric actuators adjust the seat's tilt to maintain parallelism with the ground. Additionally, the wheels, attached to the chair's chassis, are lifted by the actuator's push, providing necessary clearance for the tracks during both ascent and descent of stairs as shown in Appendix A: Detailed Information and Calculations [1].

3.9 Chassis

The chassis of the system is the main structure of the wheelchair that all the major components will mount to. The dimensions chosen for the base of the chair were 0.550m by 0.530m. The material that was chosen for the chassis was 6061-T6 square tubing. With the max stress calculated as 998psi, it can be compared to the allowable stress of 13,333 psi that the tubing material can handle. From this calculation, a 1" square tubing with ¼" thickness made of 6061 aluminum can be used without any concerns even if the wheelchair is loaded with more weight (total factor of safety of 40). The length of each support beam is calculated, and, using the length of the cylinder, the exact angle where the cylinder needs to be mounted is calculated. A CAD of the chassis is shown in Appendix B: Bill of Materials and Part References. FEA was done to ensure that the handwritten calculations were accurate, and that the chassis could handle the loading it expects [1]. The FEA results for the stresses experienced can be seen below in Appendix B: Bill of Materials and Part References.

3.10 Electronics

The component selection for the wheelchair prioritized functionality, safety, and reliability, especially for users with limited mobility. A 24V battery system was chosen to meet the high torque requirements of the motors, ensuring durability and effectiveness for daily use and obstacle navigation. To support the wheelchair's self-balancing and stair-climbing features, gyroscopes and inclinometers, specifically the SCL3300-D01-1 and IIS2DHTR accelerometer, were selected for their precision in orientation and descent monitoring. The STM32F767ZI microcontroller was picked for its compatibility with peripherals and robust control capabilities. Battery capacity calculations, considering all connected components' power needs, led to choosing a 35Ah, 12V battery from Fortress Scooters, providing more than the necessary power for extended use. This strategic selection process ensures the wheelchair is a reliable, safe, and efficient mobility aid, tailored to overcome the challenges faced by its users [1].

3.11 Software and control

The wheelchair's design incorporates two distinct operational modes, navigation and stair climbing, to cater to varying mobility needs. For navigation, a joystick was chosen over arrow buttons for control due to its intuitive design and ease of use, especially important for users with limited hand dexterity. This control mechanism allows for a dynamic range of movement, with the joystick's position dictating the speed and direction of the wheelchair through calculated radius and angle ratios. These calculations adjust the power distribution between the wheels, enabling smooth and responsive maneuvering. In stair climbing mode, the focus shifts to maintaining the user's safety and comfort by adjusting the seat angle in response to changes in orientation detected by gyroscope sensors. Actuators fine-tune the seat's angle based on continuous feedback from these sensors, ensuring the chair navigates stairs efficiently and returns to a normal position once the climb is complete. This dual-mode functionality enhances the wheelchair's versatility, making it a capable companion for overcoming everyday mobility challenges [1].

4.0 Final Design

4.1 Final Design/Modifications from the Original Design

As manufacturing began, issues with the original design arose. To move forward with the manufacturing process and solve issues, design changes needed to be made. There were major design changes to the track system, chassis, angling mechanism, turning system and minor changes to the electrical system.

4.1.1 Track System

The most important change from the original proposed design to the final design was the use of a mono-track system. The original design consists of a two-track system similar to what is found on a tank. However, purchasing a suitable track set would have led to violation of the budget constraint and no sponsorship was possible for these components. Instead, a mono-track system was chosen as the only cost-effective alternative to the two-track system originally envisioned. The two tracks can be seen below in Figure 1.



Figure 1: a) original two track system [3] b) mono-track system used.

The introduction of the mono-track also led to several new design challenges including the use of two motors on a single drive gear, the added length and height of the new track, and the struggle to turn the device with a mono-track. This single change resulted in a domino effect, leading to the redesign of all mechanical subsystems for compatibility with the mono-track as well as a pivot in the overall device design and use case from a stair-climbing wheelchair replacement to an all-terrain wheelchair attachment to better suit the new track dimensions.

4.1.2 Angling Mechanism

The change in the angling mechanism was due to the desire to use only one electric actuator instead of two to save costs and the desire to reduce the height of the overall system. In the original design, the electric actuator was mounted vertically and connected to the chassis as seen below in Figure 2.

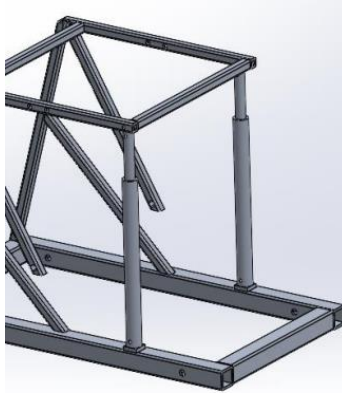


Figure 2: Initial Hydraulic orientation.

However, with this orientation, the chassis is forced to be as tall as the retracted length of the actuator. This proved to be an issue as the additional height from the new track set made the overall structure too high. To solve this issue, the electric actuator was designed to be mounted horizontally. This would eliminate the extra height created by the cylinder. The angling of the seat will still be achieved by having the actuator push against the chassis as seen highlighted in red below in Figure 3. Since these “arms” will be fixed during angling as explained in 4.1.3 Turning System, the actuator will be forced to rotate about the point highlighted in green in Figure 3. This occurs as the actuator pushes at a higher point (the red) than the point of rotation (the green). This difference in height created a moment around the point of rotation which allows the top base to angle. Since the seat is connected to the top base, the seat will also angle.

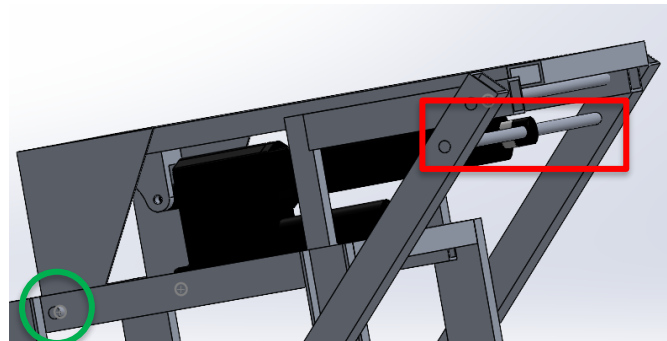


Figure 3: Angling Mechanism

Finally, the shaft highlighted in red in Figure 3 will experience a large amount of bending. This is due to the fixed supports of the shaft being further away from the point that experiences the bending. Since the shaft is forced to be 0.5in diameter due to the mounting with the actuator, both steel and aluminum solid shafts will not be strong enough and will deform through bending. This hypothesis was confirmed through testing. To overcome this issue, hardened chains rated for 2000lbs were used to connect the actuator to the chassis as seen in Figure 4 below.



Figure 4: Chain connection to chassis.

By using chains, the system now had flexibility to move a little due to the nature of chains as well as reducing the distance between the support points and the point the actuator pushes on. This allows for the actuator to push with its full 2000lbs of force without bending the chains. This was confirmed due to testing and visually confirming no bending of the chains.

4.1.3 Turning System

The biggest hurdle introduced by the change to the mono-track system was the loss of the simple turning mechanism provided by the dual track system. The original design allowed for on the dime turning with one track rotating forwards while the other rotated backwards. With just a single track, this was no longer an option. The single track allowed only for forward and backward motion. Furthermore, any turning mechanism would have to drag the track from side to side, requiring an immense amount of force due to its heavy weight, high coefficient of friction, and large surface area. All the qualities advantageous to obstacle navigation became obstacles when turning was required. The solution to address this was twofold. First was adding an additional capability to the angling mechanism to angle the track system. Second was to control castor wheels directly from the wheelchair wheels, using them to steer the device.

4.1.4 Chassis

Due to the track system being changed from a dual track system to a single-track system, the original designed chassis was unable to be used. This is due to the change in mounting points and mounting locations. In the original design the track system could directly be connected to the chassis square tubing as seen below in Figure 5.

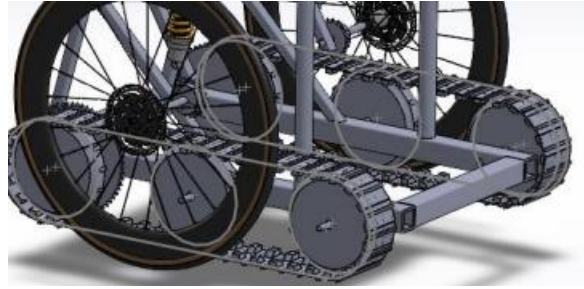


Figure 5: Initial Chassis Track Configuration

However, since the new track has a built-in suspension, the two mounting points were located on the suspension as seen below in Figure 6. This meant that two beams needed to be used to bolt into the suspension mounting points on either side as seen in Figure 6.



Figure 6: New Chassis Track Configuration

The second external change that affected the design of the chassis was the angling and turning mechanisms. Since the angling and turning mechanism needed a specific architecture to allow for desired functionality as explained in 4.1.2 Angling Mechanism and 4.1.3 Turning System respectfully, the chassis had to be designed with the necessary architecture. This meant that there were two main bases on the chassis. The first base is fixed to the track while the second base is free to angle while also supporting the seat.

Finally, a support structure had to be added to hold the motors in place. This structure as seen in Figure 7 is so the motors can be rigidly mounted onto the chassis and withstand the high torque forces it will experience during operation.

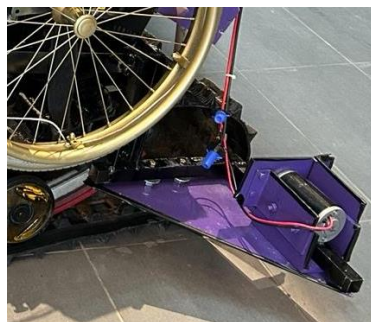


Figure 7: Motor Mounts

The entire chassis after incorporating the necessary structures for track mounting, angling mechanism, turning mechanism and motor mounting as well as the wheelchair mounted onto the angling base can be seen below in Figure 8.



Figure 8: Complete Chassis

4.1.5 Electrical System

The electrical subsystem was designed to be able to fully support the CMD's operation under both nominal and peak load conditions while ensuring the connections are secured and properly insulated due to the high current amounts being drawn. Concurrently, time was spent ensuring the connections are flexible enough to allow for easy access and removability when needing to charge the batteries or disassemble the motor subsystem for mechanical testing.

4.1.5.1 Motor Reselection

Due to communication issues with the manufacturer, the high torque motors that were initially chosen for the drivetrain were substituted with brushed DC motors supplied by Vex Robotics. The motors shown in Figure 30 in Appendix B below are chosen to be able to handle torque loads of up to 100 Nm each when coupled with a planetary gearset.

Figure 46 in Appendix C below shows the manufacturer provided drawing and specification sheet for the CIM motor, with the most relevant information from an electrical standpoint being that that motors will each have a nominal current draw of 27 A during normal operation and a draw of 67.9 A under its maximum capable load. The motors are also powered by 12 V DC as opposed to 24 V DC which were the requirements for the original set of motors. Due to the high current requirements of this system, a sufficiently robust electrical harness is needed to ensure safety during critical operating conditions. Thus, 8-gauge sized wire was used for creating the main powerlines connecting the motors and batteries to the selected Talon SRX H-bridge motor controllers shown in Figure 31 in Appendix A. The Talon SRX H-Bridge was selected, also from the Vex Robotics vendor, due to its compatibility with the power characteristics of the chosen

motors. The manufacturer provided specification sheet lists the Talon's nominal voltage input as 12 V DC and continuous current output as 60 A, which pairs well with the motors based on the power characteristics described previously [4]. Moreover, the Talons offer bidirectional control of the motors with only a single PWM signal required from the microcontroller board for both speed and direction control.

4.1.5.2 Battery Connections and Power Requirements

The only change made to the power electronics section of the subsystem compared to the initial design is regarding the connection topology of the 12 V batteries being used. Initially 24 V DC was required due to the power requirements of the previously chosen motors meaning two batteries would have been connected in series, however, since the new motors only need 12 V DC each the batteries were instead decided to be connected in parallel to each other. This increases the overall operation time of the device.

4.1.5.3 Microcontroller Board and Voltage Regulator Design

Another change made to the electrical design was that the selection for the microcontroller board used to program the overall CMD was revised to an Arduino Mega 2560 board as opposed to the STM32 Nucleo board chosen earlier. This decision was made after the first board was found to have poorer quality chips prone to shorting whereas the Arduino is more robust and was also readily available to continue prototyping. The Arduino Mega, shown in Figure 9 below, has a recommended input voltage range of 7-12 V according to its specification sheet, which means that it could be powered directly from the 12 V batteries being used on the CMD [5]. However, since the Arduino board actually operates on 5 V DC only, an onboard voltage regulator (or DC to DC buck converter) is employed to first step down any input voltage above 5 V before being passed onto the rest of the Arduino board peripherals [5]. However, to reduce the load on the Arduino's own voltage regulator and prevent overheating, an external regulator was selected to first step down the 12 V DC battery output to around 7 V DC which would then be input to the Arduino.



Figure 9: Arduino Mega 2560 Board [5]

The buck converter chosen to step down the voltage externally before the Arduino board was the LM317 3-terminal adjustable voltage regulator manufactured by Texas Instruments. This regulator was chosen as it is able provide a current up to 1.5 A over a 1.25 V to 37 V output voltage range [6]. It is also fairly simple to set the output voltage as all that needs to be adjusted are two external resistor values, R_1 and R_2 , such that placing them in the configuration shown in Figure 10 below gives the desired voltage. The numerical values for the resistors are found based on the ratio in equation (1) below [6]:

$$V_{out} = 1.25 * (1 + \frac{R2}{R1}) \quad (1)$$

where V_{out} is the output voltage resulting from the chosen $R1$ and $R2$ values.

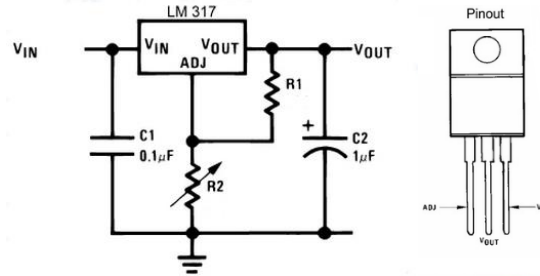


Figure 10: LM317 Adjustable Voltage Regulator Pinout and Resistor Diagrams [6]

Thus, to get a voltage of approximately 7 V to input to the Arduino board, the resistor values chosen using equation (1) above were $R1 = 1K \Omega$ and $R2 = 4.7K \Omega$. Using these resistors in the configuration above gives an output of about 7.125 V DC. As can be seen in Figure 10 above there is also a 0.1 μF capacitor present between the V_{in} /ground and a 1 μF capacitor between the V_{out} /ground connections. These are present to avoid fluctuations in the voltage signal output from the LM319 regulator [6].

4.1.5.4 Electronics for the Angling Mechanism

The main device actuating the angling mechanism is the PA-17-8-2000-POT Linear Actuator, shown in Figure 11 below, which is manufactured and sold by Progressive Automations. This is a linear actuator with an 8-inch stroke length, a lifting force of up to 2000 pounds and features a 0 - 10K Ω range potentiometer based positional feedback [7]. These specifications fit the objectives for angling the CMD up on steep inclines. This model is also 12 V operable with a nominal current draw of 20 A as opposed to 24 V for the previous selection [7]. However, as is to be expected, given that the actuator is extended by a motor housed inside there is need for an H-bridge controller board for bidirectional control to both extend and retract the actuator. Thus, the BTS7960 controller board, shown in Figure 11 was selected due to its cheapness and availability, as well as due to its 6 V - 27 V input and 43 A output range capabilities, making it the perfect option to operate the linear actuator during continuous loading times [8].



Figure 11: PA-17-8-2000-POT Actuator [7] and BTS 7960 Dual H-Bridge motor controller [8]

4.1.5.5 Sensors and User Controls

The CMD is mostly a user operated device in its current iteration, however, the angling mechanism driven by the linear actuator is automated during ascents/descents on high enough inclines for user safety and comfort. Thus, to provide angular state feedback for the seat subframe a single ICM20948 inertial measurement unit (IMU) was used. This is a deviation from the initial design since three sensors were estimated to be required for full state feedback, however, the

only required information is the angle of the seat relative to the ground, which the single IMU mounted to the side of the seat frame is able to provide, to correct the orientation of the seat to a relatively upright position. This sensor has very small power requirements and is therefore powered by the Arduino board.

The user's main form of control over the wheelchair is using two joysticks mounted on either arm of the chair. These are both low power peripherals as well and are thus powered by the Arduino board as well.

4.1.5.6 Fuses and Circuit Breaker

Finally, the safety of the electrical components themselves is to be considered. Since this is a high-powered application and high amounts of current are drawn from the lead acid batteries being used, there is a possibility of current surges frying out critical electrical components. Thus, each major electrical component connected to the batteries is connected to a fuse rated for the appropriate current value first. The list of fuses used is summarized in Table 2 below. An emergency disconnect switch was also installed as a safety option for the user to cut the current draw for all of CMD.

Table 2: Fuses Used

Electrical Component	Fuse Rating	Number of Components
CIM Motor	70 A (fast blow)	2
PA-17 Linear Actuator	20 A (fast blow)	1
Arduino Mega	1 A (fast blow)	1

4.1.6 Code Architecture

The final software design included the use of two joysticks for controlling the movement of the overall device as well as the tilt angle of the seat. There were multiple changes from the initial software design that was previously devised. The device is controlled mainly through two joysticks, one at each armrest.

Firstly, the logic for movement and speed control was changed due to limitations from the joysticks. The values that were read from the location of the joystick did not scale linearly like they should. Instead, it was closer to a binary reading where if the joystick was pushed slightly in any direction, the reading would show it was pushed to the last point in said direction. Consequently, a linear scaling of the location of the joystick to control the speed of the motor was no longer viable. To counter this issue, one joystick was used to control the direction of movement while the other joystick was used to control speed. To control the direction of motion of the device, the user would push and hold the corresponding joystick such that it points in the desired direction. On the other hand, to control the speed, the user would nudge the other joystick in one direction to increase the speed and vice versa. The speed was controlled by introducing five "gears" so that, based on the users' nudges of the corresponding joystick, the device can move at 20%, 40%, 60%, 80%, or 100% speed. This device speed control is done by managing the speed of the drive

motors through their Talon SRX motor controllers, which take a PWM signal to control the speed and direction of the motors they are attached to. The Talon SRX treats a 1500 microsecond pulse width as the neutral position (motor stopped). Pulse widths longer than 1500 microseconds, until the 2000 microsecond maximum, increase speed in one direction, and pulse widths shorter than 1500 microseconds, until the 1000 microsecond minimum, increase speed in the opposite direction. Therefore, the speed was controlled as follows:

```
DriveMotorController.writeMicroseconds(1500 ± (100 + speed * 100));
```

Where the speed variable is an index from 0 to 4 that controls the speed in 20% intervals and the ± determines the direction of motion.

The other thing that was controlled through the code was the tilt angle of the seat. Since this wheelchair attachment is meant to give users the ability to go over steps and move on steep inclines/declines, it is necessary, for the safety and comfort of the user, to allow for the control of the seat angle. This was done by pushing/pulling the joystick that was previously used for controlling the speed of the device. Holding the joystick at a position will trigger the expansion/retraction of the linear actuator that controls the tilt angle of the seat. The controls of the joysticks are summarized in Figure 12 below.

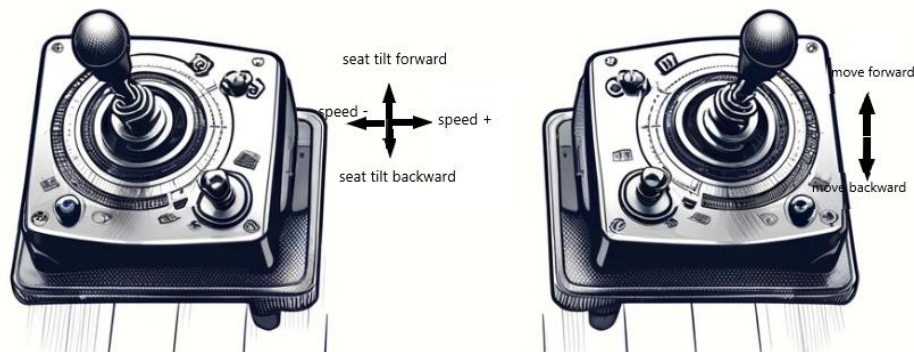


Figure 12: Labelled Joysticks Controls

As a safety precaution, if the right joystick was clicked, the motors would immediately stop while if the left joystick was clicked, the seat actuator would return to its neutral position. The full code can be seen in Appendix D: Device Code.

4.2 Construction/Manufacturing

To assemble the final design effectively and efficiently, a series of steps in how to assemble the different components was created. This was to ensure structure during manufacturing and to minimize mistakes when assembling. The bill of materials for each system can be seen in Appendix B: Bill of Materials and Part References. Drawings of the machined parts can be seen in Appendix C: As Built Drawings.

4.2.1 Track System

The mono-track system used was sourced from an old snowmobile, which was desirable for its excellent traction and integrated suspension system. The outside of the track was made of a thick rubber material with lugs for additional grip. The integrated suspension system was a combination of plastic and rubber wheels mounted on skis to fit inside of the track with solid steel supports holding the spring and damper suspension. The system provided adjustment points for appropriate tensioning and tuning once inside the track. The last piece of the mono-track was the drive gear, which was placed on the inside of the track and interlocked with the inner lugs to rotate the track while the suspension system wheels were free to rotate, keeping it in place within the moving track. The drive gear had a shaft protruding from either side, which would be coupled to the motors and gearboxes, allowing them to rotate the track using the drive gear and propel the device. The integrated suspension system and drive gear can be seen below in Figure 13.



Figure 13: integrated suspension system and drive gear.

The only major modification made to the mono-track was the addition of pin holes at the ends of the drive gear shafts to add the couplers. The aluminum shaft couplers were used to step down the one-inch drive gear shaft locked with a pin to the gearbox output shaft locked in with a set screw and keyway. The gearbox was attached to the motor through a plate, which connected it to the mounting assembly of the chassis, securing it in place and preventing rotation of the motors themselves. The mounts were assembled onto pieces of square aluminum tubing which protruded out from either side of the chassis. The assembled track system weighed 110lbs, with a length of 56", a height of 24", and a width of 18".

4.2.2 Chassis

The construction of the chassis was carried out in a sequence of steps that was order dependent. The list of all the parts needed to assemble the chassis can be seen in Appendix B: Bill of Materials and Part References. The numbers shown in this section can be correlated to the actual part in Appendix B: Bill of Materials and Part References. If the parts need to be machined, the drawings of the machined parts can be seen in Appendix C: As Built Drawings. The chassis was broken down into three main sections: the fixed base that mounted onto the tracks, the angling base that housed the wheelchair and the mechanical arms for the turning mechanism.

The fixed base was assembled first. The first step was to weld the base structure into a rectangle as shown below in Figure 14.

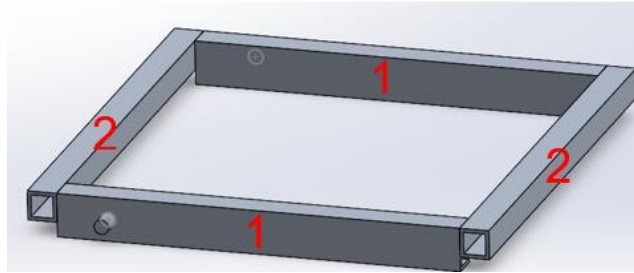


Figure 14: Step 1 Assembly

Next, the auxiliary support pieces were welded onto the rectangular base as seen below in Figure 15. This completes the welding of the bottom base.

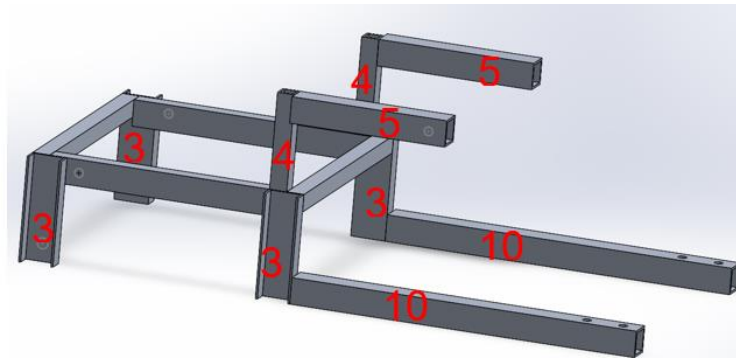


Figure 15: Step 2 Assembly

Next the upper base that the wheelchair mounts need to be made. Just like the bottom base, the first step is to create a rectangular base by welding the components together as shown below in Figure 16.

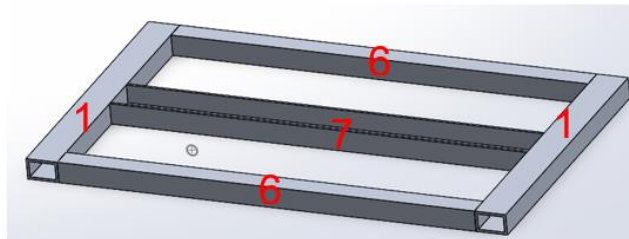


Figure 16: Step 3 Assembly

Similarly, weld the two auxiliary support pieces onto the rectangular base (piece 8). Then use the electric actuator mount (Piece 9) and bolt it as far aft on the center c-channel For. After this has been done, the base should look as shown below in Figure 17.

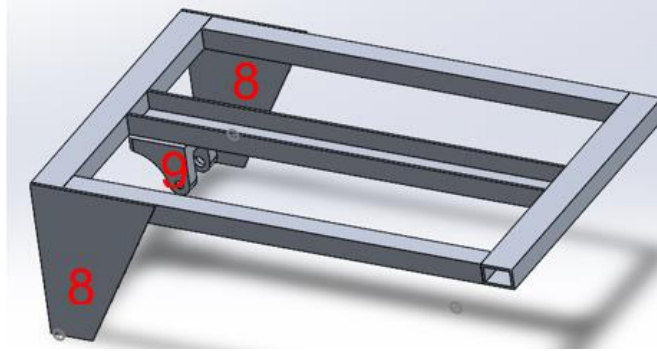


Figure 17: Step 4 Assembly

Next, the chassis component for turning is two 1.5in square tubing (piece 10) that will be used later in the assembly process. Next all the three main components can be assembled. The main base and the top base can now be assembled by putting 2 0.5in 3in long bolts (piece 11) through pieces 8 and 1. The two tubing for turning can also be assembled with 2 0.5in 5in long bolts (piece 12) through pieces 10 and 5. Next, the actuator can be installed connecting to the stock bracket (piece 9) with the given stock bolt (piece 13). After these steps, the chassis will look as shown below in Figure 18.

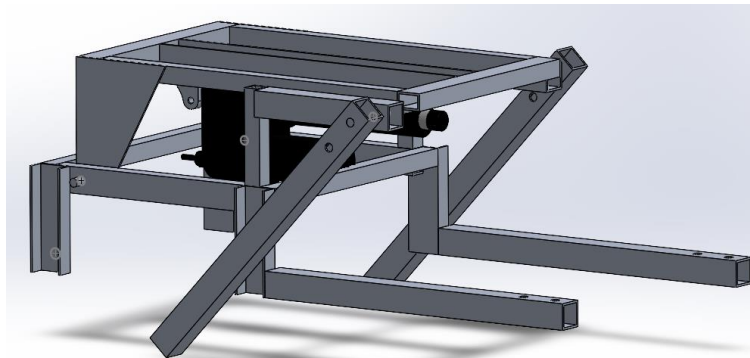


Figure 18: Step 5 Assembly

Finally, the chains can be added and routed between piece 4, the actuator and turning arms (piece 10). The chassis will then be completed, and any wheelchair can be mounted, with bolts (piece 12) onto piece 6 of the top base. This entire assembly can then be mounted onto the track suspension with 4 bolts (piece 12). The finished product can be seen in Appendix B: Bill of Materials and Part References.

4.2.3 Turning System

To overcome the obstacles surrounding turning, a new turning system was designed and consisted of two main components. First, the angling mechanism discussed in section 4.1.2 Angling Mechanism was redesigned around the mono-track such that it could angle not only the seat, but also the entire device with the pivot point at the rear of the track. This action minimizes the surface area of the track, requiring less force to turn the device. This was accomplished using the “arms” mentioned in section 4.1.2 Angling Mechanism. The arms work in conjunction with the linear actuator to achieve both seat angling and track angling depending on the actuator position.

As previously discussed, a system of chains was used for the seat angling. The chains were tensioned through the extension of the actuator, with full tension locking the extension of the arms and instead forcing the seat to rotate as it is mounted onto a freely rotating base. To angle the track, an opposing system of cables was added that would tension as the actuator retracted. The cables coupled the arms to the eyelets seen on the step in the front of the track. Once sufficiently tensioned through retraction, the arms would rotate down into the ground, pushing the front of the track into the air. Due to the immense holding force of the actuator, this system would not move after being set into position.

The second vital component of the new turning system was the wheel control mechanism. This system was inspired by the turning system used by snowmobiles where the forward propulsion comes from the track system in the rear, while a set of skis in the front are used to steer the device side to side. The castor wheels mounted at the bottom of the arms are the device's replacement for skis which are more suitable for the variety of expected terrain. Once the arms are fully retracted, most of the device weight is placed on these wheels and the rear edge of the track remains in contact with the ground. The castor wheels complete with their mounting assembly were taken from a wheelchair and bolted to the bottom of the arms to achieve the desired height upon full retraction. To control the steering wheels, a braided steel cable like the tension cable for the angling mechanism was routed through the steering wheel assembly and attached to each wheelchair wheel at two points. The result was a cable that could be tensioned in either direction by rotating the wheelchair wheels either forwards or backwards, holding the steering wheels at the desired angle of turning. The benefits of this design were its simplicity and cost-effectiveness, as well as ease of use for a rider already accustomed to turning in a wheelchair.

4.2.4 Electrical System

While the commissioning section below goes into detail over individual pin connections and logic required for unit testing of the electrical subcomponents, Figure 19 below shows the full electrical schematic employed for creating wired connections on the CMD.

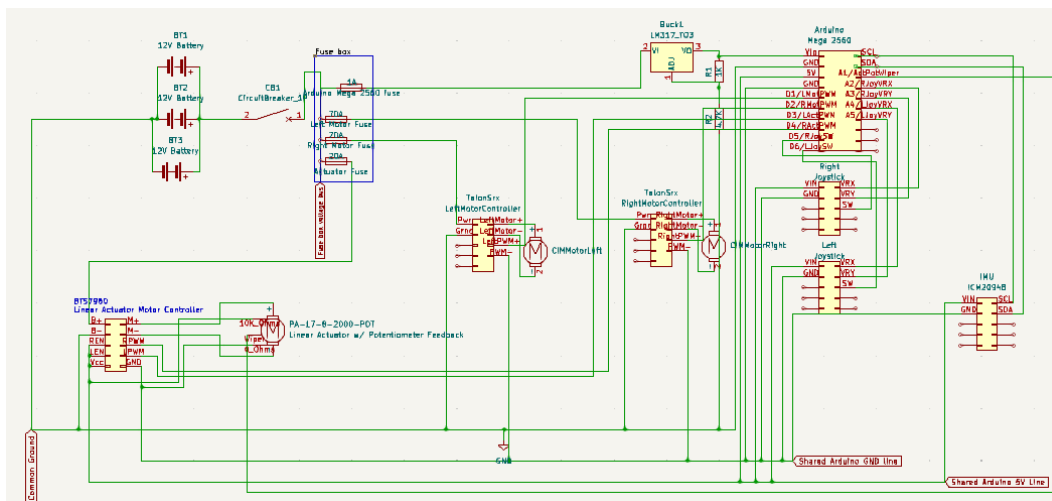


Figure 19: Full Electrical Schematic of the CMD

This entire schematic was implemented physically, with particular attention being devoted to ensuring electrical safety and the integrity of connections, given the system's operation at high currents. Recognizing the challenges posed by handling large wire gauges, especially 8-gauge wires fundamental in the design due to their capacity to handle high current loads, meticulous methods were employed in making secure connections. Splicing, a critical technique in the electrical assembly, was executed with precision. Initially, wires were carefully joined using soldering methods to ensure a robust and conductive bond, followed by the application of heat shrink tubing. This not only insulated the splice but also provided additional protection against mechanical wear and environmental factors.

To further enhance the reliability of connections and facilitate maintenance, various crimping techniques were utilized across different sections of the assembly. Crimped connections offer the dual benefits of mechanical robustness and good electrical contact, essential for the long-term stability of the system. Specifically, for joining 8-gauge wires, winged wire connectors were chosen for their ease of use and effectiveness in creating a secure, insulated splice capable of withstanding the system's electrical demands. This choice of connectors and crimping methods reflects a commitment to constructing a system that prioritizes safety, efficiency, and durability, adhering to the highest standards of electrical engineering practices. Images of the connections and electrical assembly are shown in Appendix B: Bill of Materials and Part References.

4.3 Commissioning

The testing of the electrical subsystems before full integration was crucial to ensure proper functionality of the CMD and to reduce time spent troubleshooting and debugging once fully connected. Since individual components are tested for proper operation beforehand, certain possibilities can be ruled out when problems do arise as there is already some understanding of the individual subcomponents used as part of the overall whole.

4.3.1 Motor Control Testing

The motor control was tested by connecting a digital pin on the Arduino to a single Talon's PWM line and then outputting a signal value from 1000 to 2000 to control a CIM motor. From experimentation it was determined that the 1500 mark is where both the motors stop, with values greater than 1500 driving the motors forward and less than 1500 driving them backwards. It was also confirmed that the motors have higher RPM outputs the further their PWM signal is from the 1500 mark.

Due to the high torques experienced at the driving shaft of the track set, both motors, stepped up with the planetary gearboxes, were decided to be coupled to the same singular driving shaft on the tracks. This means that the motors are connected with their spin direction polarized. Thus, through testing it was found that when both motors are coupled to the same shaft, they can be used to spin it in the same direction when equal and opposite PWM signal values are provided to each from 1000 to 2000. For example, making the right PWM signal 1700 and the left PWM signal

1300 would make the CMD go forward at 40% speed whereas making the right PWM 1200 and the left PWM 1800 would make it go backward at 60% speed.

At the same time the joystick controls were also tested by connecting the x and y direction pins to analog pins on the Arduino and the switch button pin to a digital pin. Actuating the controls in a particular direction was used to test the CMD motors PWM output.

4.3.2 Linear Actuator Control Testing

Figure 20 below shows the pin connections required for connecting the linear actuator to the BTS7960 motor controller. These connections were completed to test linear actuator extension and retraction prior to integrating the system under the CMD angling subsystem. As can be seen there are three wires next to the label 'POT' which refers to the potentiometer feedback lines from the actuator. The grey/white wire is the 0 Ω pin, the yellow is the 10K Ω pin, and the red is the 'wiper' pin, which is the connection that changes the potentiometer resistance value based on the actuator's stroke length [7]. The wiper pin is fed into an analog input on the Arduino board for the feedback.

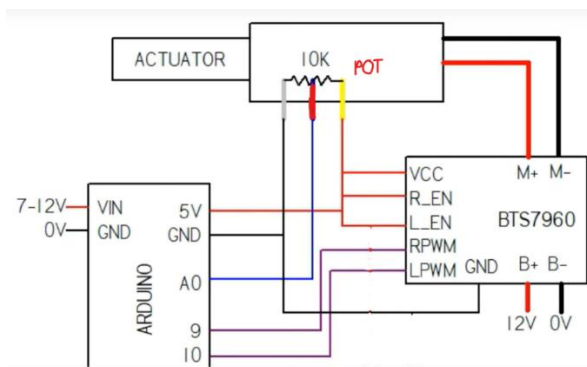


Figure 20: PA-17 linear actuator, Arduino, and BTS7960 pinout diagram [8]

Due to the full length of the rod not being entirely extendable and from how the actuator is built, however, only a small range of the 0 - 10K Ω is actually available [8]. This range was thus found by connecting the white potentiometer pin to the positive terminal on a digital multimeter and the wiper pin to the ground terminal, starting with the actuator fully retracted, noting the resistance, and then extending to full stroke length and measuring the resistance again to get the full range of values available to measure [8]. For this actuator the resistance at full retraction was found to be 502.6 - 502.7 Ω whereas the resistance at full extension read 3.687K - 3.688K Ω . The values were remapped to the 0 - 1023 analog range read by the Arduino using the following equation (2):

$$1023 * \frac{Resistance}{10K} = Analog\ Mapped\ Value \quad (2)$$

Applying the formula above gave a range of 52 to 377 from full retraction to extension respectively.

4.3.3 IMU Feedback

The ICM20948 IMU was connected to the Arduino via the SDA and SCL pins, both devices have clear labels for them, and then the ground and power for the sensor as usual. Upon implementing an Arduino library that performed real time sensor fusion, angular data was acquired. Upon connecting the linear actuator and IMU both to the Arduino, angling automation and feedback were tested with successful results. Following this the electrical harness was finalized for mounting onto the overall CMD frame.

4.4 Testing and Performance

4.4.1 Durability Test

When the wheelchair is loaded with 2000lbs load, the supporting rod that is being pushed by the actuator bent due to the large amount of bending moment. This is caused because the fixed supports are far away from the point that experience the force. This was solved by using 2000lbs rated chains instead of a rod. Then the wheelchair was tested by loading it with a 200lbs person to simulate real-world usage and the linear actuator was able to easily incline the seat to the maximum extension.

Due to repeated testing, the motor mounts bent due to the high torque from the motors. Therefore, new mounts were made from a thicker aluminum material to withstand high torque. During testing, due to a connection error, only one motor spun while the other was stationary, putting significant torsion on the motor shaft which led it to snap off. It was later fixed by welding it directly to the coupler connecting the drive shaft.

4.4.2 User comfort and safety

Volunteers and team members used the wheelchair for an extended period, reporting high comfort levels and all safety systems performed flawlessly during the test.

4.4.3 Control system

A group of volunteers and team members with varying levels of mobility navigated a predefined course, providing feedback on the joystick controls. They were all positive feedback on the ease of use and responsiveness.

5.0 Scheduling and Budget

5.1 Schedule

In the past 3-4 months, the team had been achieving milestones and working towards completing the project. A rough outline of the schedule and project timeline can be seen in Figure 21 below.

Project Timeline 2024

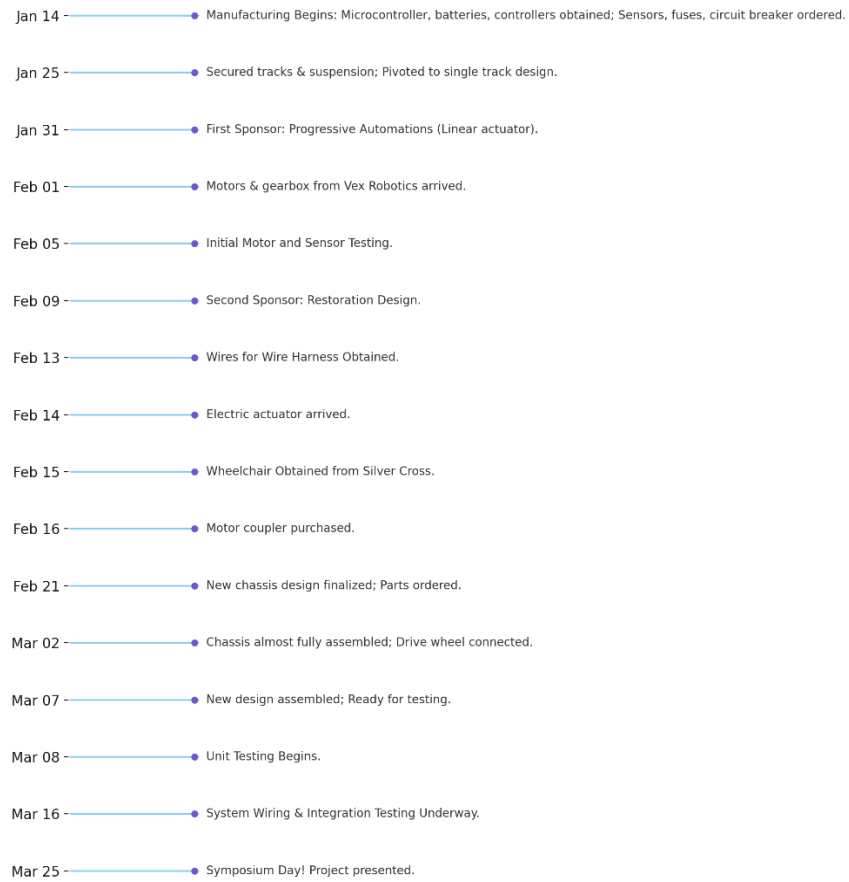


Figure 21: CMD Project Timeline in 2024

More details about the timeline, as well as accompanying photos and videos for components, testing, and more, can be seen on the blog page CMD's website [9].

5.2 Original Expected Budget

The original budget was divided into electronics, mechanical and fabrication costs. This budget can be seen below in Table 3.

Table 3: Budget for materials [1]

Expenses	Number of Units	Cost Per Unit (\$)	Budget Allocated (\$)
Electronics			
Microcontroller*	1	\$16.26	\$20.00
DC Motors	2	\$190.99	\$400.00
Sensors	3	\$73.71	\$75.00
Linear Actuators	2	\$195.00	\$350.00
Battery	2	\$122.99	\$300.00
Mechanical Hardware			
Treads and Track Wheel set	1	\$2158.30	\$2500.00
Suspension	2	101	110
Sheet Metal (Aluminum)	2 square feet	\$9.39	\$50.00
Fasteners and Misc*	N/A	N/A	N/A
Fabrication			
Labor**	N/A	N/A	N/A
Total	N/A	\$3552.37	\$3905.00

* These components are either provided by the school or are available from one of the group members.

** Labor for using the EMS should be 0 as the parts machined will require less than 30 minutes.

5.3 Actual Spent Budget

The budget table was revised once manufacturing was completed. The new budget was divided into electronics, mechanical, and fabrication costs. The total expenses can be seen below in Table 4. The actual amount spent was \$2611.44, which is \$940.90 under the initial expected cost.

Table 4: Final Amount Spent

Expenses	Total Cost (\$)	Notes
Electronics		
Arduino & Motor Controllers	\$37.28	Actuator controller bought. Arduino and motor controllers were free
Motor and Gearboxes	\$494.74	Includes, motors, gearboxes and shafts
Actuators, wires & Battery	\$0	Sponsored
Electrical Parts/Misc	\$134.96	Connectors, contacts, fuses
Mechanical Hardware		
Tracks and Suspension set	\$725	Drive gear, track and suspension
Wheelchair	\$0	Sponsored
Chassis/mechanical Components	\$731.82	Materials, wheels, spare parts etc
Fasteners and Misc	\$352.64	Fasteners, chains, spray paint etc
Fabrication		
Labor	\$135	Machining from E3
Total	\$2611.44	

6.0 Conclusions and Recommendations

This device was created to give people with limited to no use of their legs the mobility aid they need to navigate the world. The final design features a single track with an integrated suspension system to absorb shocks and help users go over things like bumps and train tracks. It also has a linear actuator that handles the seat angling for safety and comfort and aids in the turning mechanism. Finally, the software, along with the wiring and electronics, allow the user to control the device components efficiently and accurately, leading to overall smooth operation.

Naturally, this project has served as both a valuable learning opportunity and a catalyst for identifying areas for design improvement. Some design choices were necessitated by time constraints while others were made due to the limited budget. For subsequent iterations or enhancements, we suggest adopting a dual, smaller track system. This approach is expected to lower the system's overall height and simplify the device's turning mechanism.

7.0 Teamwork

7.1 Teamwork Efficiency/Breakdown

For a project of this scale, an efficient team structure was necessary to bring the vision of CMD to life. The project was broken up into its main subsystems and a primary and secondary member were assigned to each subsystem. Because of the demanding mechanical and manufacturing workload, more members were required to contribute to these components of the project. Otherwise, group members were allocated to the subsystems best suited to their skillset to ensure that the project subsystems could be completed as quickly and efficiently as possible to begin integration testing.

7.2 Task Completion of Each Member

To complete the manufacturing of the project, each team member needed to successfully complete tasks. The task breakdown of what each member did was as follows:

Arshak worked on the overall assembly of the mechanical system and integration of the motors to the track system. Arshak also aided Nigel in mechanical testing and design. Abhinav worked on the entire design, construction, and implementation of the electrical system, along with electrical testing. Abhinav also aided Mohamed in code architecture and testing. Nigel worked on the redesign of the entire chassis, assembly and manufacturing of the mechanical components and aided Arshak in the mechanical integration and mechanical testing. Mohammed worked on the code architecture and validating the implemented code through testing. Avinash worked on design and implementation of the motor mounts and aided Nigel in machining and manufacturing.

References

- [1] N. Fernandes, A. Petrosyan, A. Gupta, M. Gasser and A. Yarram, "Capstone Report," University of Waterloo, Waterloo, 2023.
- [2] Air Canada, "Air Canada Cargo - Fleet," [Online]. Available: <https://www.aircanada.com/cargo/shipping/our-fleet>. [Accessed 3 December 2023].
- [3] Superdroid Robotics, "HD2 Pair of Molded Spliceless Tracks and Wheel Set - Generation 4," Superdroid Robotics, [Online]. Available: <https://www.superdroidrobots.com/store/robot-parts/mechanical-parts/treads-tracks/sdr-tracks-wheels/product=1607>. [Accessed 8 April 2024].
- [4] Cross the Road Electronics, "Talon SRX – User's Guide," 03 02 2017. [Online]. Available: <https://www.vexrobotics.com/217-8080.html>. [Accessed 02 2024].
- [5] Arduino, "Arduino Mega 2560," 16 12 2020. [Online]. Available: <https://store-usa.arduino.cc/products/arduino-mega-2560-rev3?selectedStore=us>. [Accessed 02 2024].
- [6] Texas Instruments, "LM317 3-Terminal Adjustable Regulator," 04 2020. [Online]. Available: <https://www.ti.com/lit/ds/symlink/lm317.pdf>. [Accessed 02 2024].
- [7] Progressive Automations, "Heavy Duty Linear Actuator PA-17," 06 2020. [Online]. Available: <https://www.progressiveautomations.com/products/heavy-duty-linear-actuator>. [Accessed 02 2024].
- [8] Science Fun, "Arduino Linear Actuator Position Control," Science Fun, 03 02 2022. [Online]. Available: <https://www.youtube.com/watch?v=c7JtfogOsTQ&t=392s>. [Accessed 02 2024].
- [9] M. Gasser, "CMD," CMD, [Online]. Available: <https://cmd-business.webflow.io/>. [Accessed 8 April 2024].
- [10] CCL Industrial Motor Limited, "CIM Motor Vex Robotics," 2023. [Online]. Available: https://www.vexrobotics.com/217-2000.html#attr-vex_docs_downloads. [Accessed 7 March 2024].

Appendix A: Detailed Information and Calculations

This appendix will contain all detailed calculations and supporting information that will help provide further information to support the initial design.

The initial track design can be seen below in Figure 22

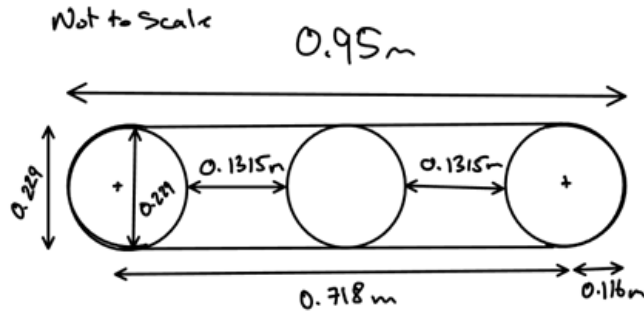


Figure 22: Initial Track Design

Below in Figure 23, is the designed drive chain mechanism.

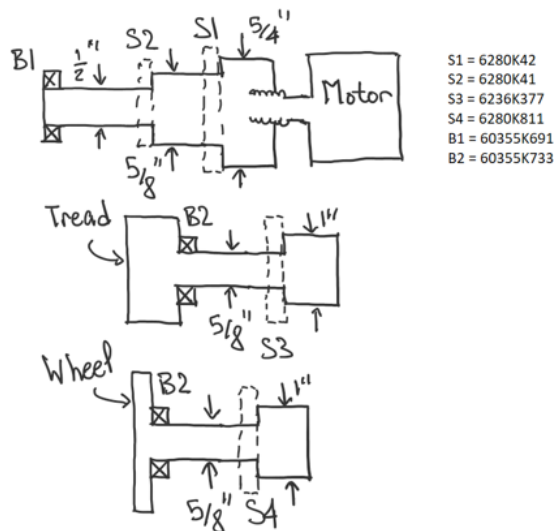


Figure 23: Initial Powertrain System

To select motors, hand calculations were carried out. The worst-case scenario free body diagram can be seen below in Figure 24.

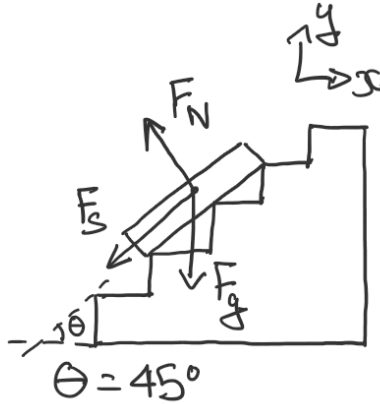


Figure 24: Worst Case Free Body Diagram

Based on the free body diagram in Figure 24, the torque that was required was calculated as shown below.

$$T_L = F * d$$

$$T_L = \left(\frac{\sqrt{2}}{2} \mu_s F_g + \frac{\sqrt{2}}{2} F_g \right) * d$$

$$T_L = \frac{\sqrt{2}}{2} (190kg) \left(\frac{9.81m}{s^2} \right) (0.91 + 1)(0.25m)$$

$$T_L = 629.33Nm$$

Next the speed that the motor can provide can be seen calculated below.

$$v = \Omega * r$$

$$v = \frac{115rpm * 2\pi rad/rot}{60s/min} * 0.35m$$

$$v = \frac{4.215m}{s}$$

$$v = 14.4km/h$$

$$MA = \frac{Effort\ Arm\ Length}{Load\ Arm\ Length} = \frac{0.1}{0.05} = 2$$

$$F = \mu * N = 0.6 * 1334 = 800.4N$$

$$Torque = F * R = 800.4 * 0.03 = 24\ Nm$$

$$F_{pivot} = \frac{T}{Brake\ Lever\ Length} = \frac{24}{0.15} = 160\ N$$

Where F_{pivot} represents the force that the user needs to apply to the brake level to generate the required torque [1].

$$Actual\ Pivot\ Force = 160 * 1.5 = 240\ with\ a\ safety\ factor\ of\ 2$$

Next, the suspension was analyzed to determine a suitable shock absorber as shown below.

$$Load\ per\ wheel = \frac{total\ weight\ of\ the\ wheelchair\ and\ user}{Number\ of\ wheels} = \frac{500lbs}{2} = 250lbs\ or\ 113.4kg$$

$$\text{Spring constant } (k) = \frac{1134N}{25} = 45.36 \text{ N/mm}$$

The damping constant is important for controlling the speed at which the spring compresses and rebounds [1].

$$\text{Mass per wheel} = \frac{1134N}{9.81} = 115.6 \text{ kg}$$

The natural frequency (ω_n) is given by $\omega_n = \sqrt{\frac{k}{m}}$

$$\omega_n = \sqrt{(4536/115.6)} = 6.275 \text{ rad/s}$$

$$\text{For critical damping } c = 2 * \omega_n * m = 2 * 6.275 * 115.6 = 1450.78 \text{ Ns/m}$$

Then the angling mechanism was analyzed based on the diagram shown in Figure 25.

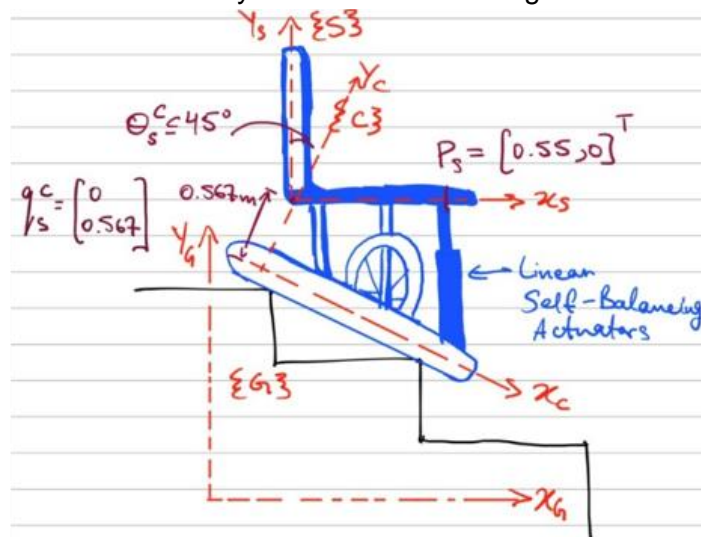


Figure 25: Angling Mechanism Reference Frame

2D transformation matrix from seat frame (X_s) to chassis frame (X_c) [1].

$$G_s^c = \begin{bmatrix} R_s^c & g_s^c \\ 0 & 0 & 1 \end{bmatrix} = \begin{bmatrix} \cos 45 & -\sin 45 & 0 \\ \sin 45 & \cos 45 & 0.567 \\ 0 & 0 & 1 \end{bmatrix} = \begin{bmatrix} \frac{\sqrt{2}}{2} & \frac{-\sqrt{2}}{2} & 0 \\ \frac{\sqrt{2}}{2} & \frac{\sqrt{2}}{2} & 0.567 \\ 0 & 0 & 1 \end{bmatrix}$$

Finding the point $P_s = \begin{pmatrix} 0.55 \\ 0 \end{pmatrix}$ in plane X_c to determine the length of the stroke of the actuator needed.

$$P_s^c = G_s^c P_s = \begin{bmatrix} \frac{\sqrt{2}}{2} & \frac{-\sqrt{2}}{2} & 0 \\ \frac{\sqrt{2}}{2} & \frac{\sqrt{2}}{2} & 0.567 \\ 0 & 0 & 1 \end{bmatrix} \begin{bmatrix} 0.55 \\ 0 \\ 1 \end{bmatrix} = \begin{bmatrix} 0.389 \\ 0.956 \\ 1 \end{bmatrix}$$

To calculate the minimum force each actuator must exert, it's crucial to examine the force equilibrium. With an assumption that a 300lbs load is to be evenly distributed across two actuators, each actuator would be required to support half of this total load. [1].

Summing all the forces in the x-axis:

$$\sum F_x = 0 \text{ (No forces in x direction)}$$

Summing all the forces in the y-axis:

$$\begin{aligned} \sum F_y &= 0 \\ R_A + F_1 - W &= 0 \\ R_A + F_1 - 150 &= 0 \\ R_A + F_1 &= 150 \end{aligned}$$

Moment about point A:

$$\begin{aligned} \sum M_A &= 0 \text{ (Counterclockwise being positive)} \\ -W(0.275) + F_1(0.389) &= 0 \\ F_1 &= 106.04 \text{ N} \end{aligned}$$

$$R_A = -43.96 \text{ N (Acting in opposite direction to the assumed direction)}$$

The chassis material needed to be determined and so a Material Selection Analysis was done based on the free body diagram shown in Figure 26 below.

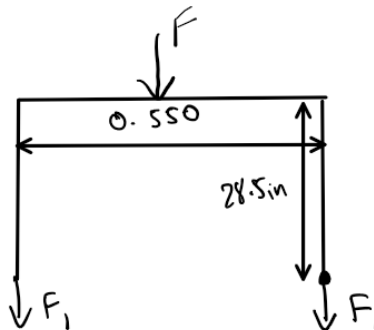


Figure 26: Chassis Free Body Diagram

The force per support is calculated as below:

$$F = \frac{265 \text{ lbs}}{4 \text{ supports}} = 66.25 \text{ lbs/support}$$

Bending moment was then calculated as shown below:

$$\begin{aligned} M_{max} &= F \cdot d \\ M_{max} &= 66.25 \cdot \left(\frac{28.5}{12}\right) \\ M_{max} &= 157.344 \text{ ftlbs} \end{aligned}$$

The maximum stress that the material undergoes can be determined according to the specific material selected. In this case, the material is 1in square tubing made of aluminum 6061-T6 with a thickness of 1/4in. To compute the maximum stress, the moment of inertia for the square tubing needs to be calculated using the following formula. [1].

$$\begin{aligned} I &= \frac{l_{outer}^4 - l_{inner}^4}{12} \\ I &= \frac{1^4 - (1 - (2 \cdot 0.25))^4}{12} \\ I &= 0.0781 \text{ in}^4 \end{aligned}$$

This was done with the formula below where M is the max moment calculated above, y is the distance from the outer beam to the neutral axis of the beam and I is the moment of inertia calculated above [1].

$$\sigma_{max} = \frac{M \cdot y}{I}$$

$$\sigma_{max} = \frac{154.344 \cdot 0.5}{0.0781}$$

$$\sigma_{max} = 988psi$$

The maximum stress determined through calculations can be evaluated against the permissible stress that the tubing material is capable of withstanding. By applying a safety factor of three, the allowable stress for the tubing material, specifically 6061 Aluminum with a maximum yield strength of 40,000 psi, can be derived using the formula provided below [1].

$$\sigma_{all} = \frac{40000psi}{3}$$

$$\sigma_{all} = 13333psi$$

Next, the chassis supports were analyzed. The supports along with current known measurements can be seen below in Figure 27.

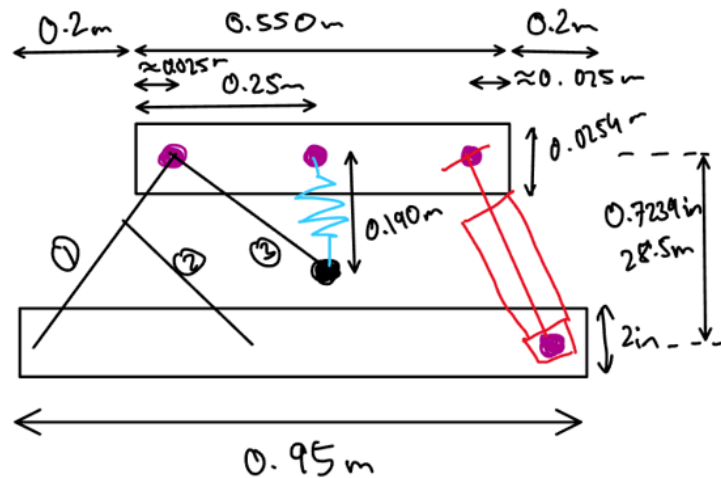


Figure 27: Initial Chassis Measurements

The angles created from the supports can be seen summarized in Figure 28 below.

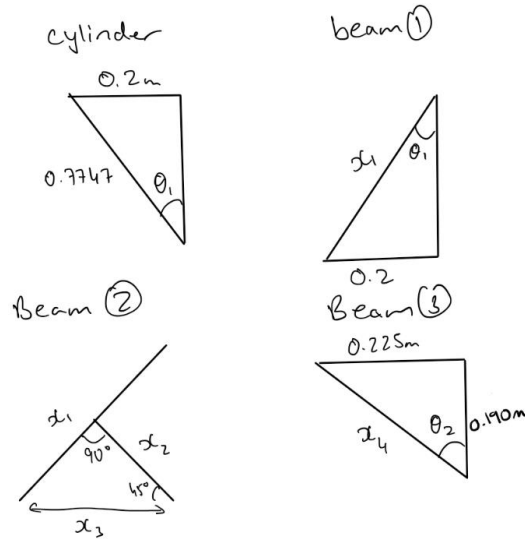


Figure 28: Support Member Angles

First the angle at which the cylinder needs to be mounted can be calculated as shown below.

$$\theta_1 = \sin^{-1}\left(\frac{0.2}{0.7747}\right) = 14.96^\circ$$

Having identified all the necessary parameters for beam one, which precisely mirrors the cylinder in terms of angle, we can infer that the beam's dimensions will match those of the cylinder by direct observation. With the value for x_1 established, we are now in a position to calculate the values for x_2 and x_3 for the second beam. This calculation is based on the assumption that the beam is attached at the midpoint of x_1 and extends at a 45-degree angle, as detailed in the following steps. [1].

$$x_1 = \left(\frac{0.7747}{2}\right) \tan 45 = 0.3874m$$

$$x_2 = \left(\frac{0.7747}{\sin 45}\right) = 0.548m$$

Finally, x_4 and θ_2 can be solved based on the known horizontal position and length of the suspension as shown below [1].

$$\theta_2 = \tan^{-1}\left(\frac{0.225}{0.190}\right) = 49.82^\circ$$

$$x_4 = \left(\frac{0.225}{\sin 49.82}\right) = 0.294m$$

Since all the needed dimensions for the chassis supports and bases are calculated. A summary of all these dimensions can be seen in Figure 29 below.

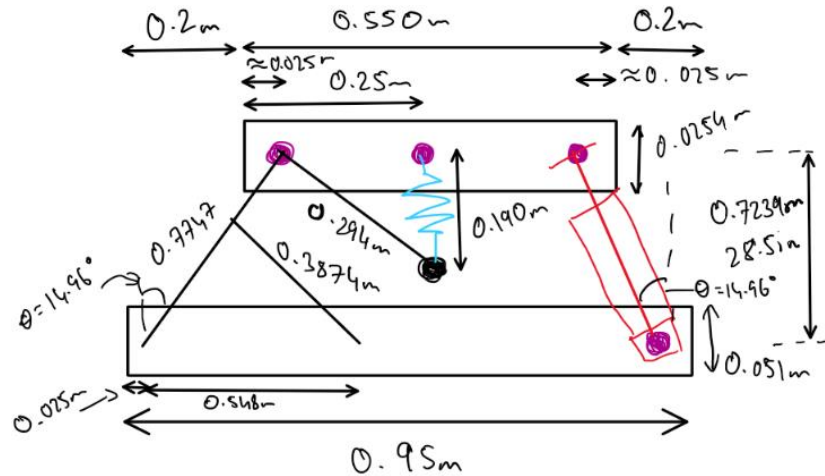


Figure 29: Summary of All the dimensions

Next the battery was determined by analyzing the amount of load it would experience. First the nominal power ratings of each component must be found to determine their watt hour requirements based on the maximum single use runtime [1]

$$Ah \text{ rating} = \frac{(P_{Motors} + P_{Actuators} + P_{Microcontroller} + P_{Accelerometer} + P_{Inclinometers}) * runtime}{24V}$$

$$Ah \text{ rating} = \frac{(2 * 24 * 10 + 2 * 24 * 0.6 + 4 * 0.1 + 3.6 * 0.000011 + 2 * 3.6 * 0.0021) * 1.39}{24}$$

$$Ah \text{ rating} = \frac{(2 * 24 * 10 + 2 * 24 * 0.6 + 4 * 0.1 + 3.6 * 0.000011 + 2 * 3.6 * 0.0021) * 1.39}{24}$$

$$Ah \text{ rating} = \frac{707.81}{24} = 29.49Ah$$

The chosen electronics can be seen summarized below in Table 5.

Table 5: Chosen Electronics

Part Name	Nominal Voltage Requirement	Nominal Current Requirement
MP36 motor (x2)	24V	10A
PA-09-12 linear actuators (x2)	24V	0.6A
SCL3300-D01-1 inclinometer (x2)	3.6V	2.1mA
IIS2DHTR accelerometer (x1)	3.6V	11µA
STM32F767ZI MCU (X1)	4V	100mA

Appendix B: Bill of Materials and Part References

All the parts that are necessary for the assembly of the chassis can be seen below in Table 6.

Table 6: Chassis Bill of Materials

Item No.	Part Type	Dimensions	QTY	Notes
1	1.5x1x0.125in Tubing	13.75 in Long	4	Drawing of part in Appendix C
2	1x1x0.0125in Tubing	16in Long	2	No drawing needed
3	2x1x0.125in C-channel	6in Long	4	Drawing of part in Appendix C
4	1x1x0.125in Tubing	5.5in Long	2	No drawing needed
5	1.5x1.5x0.125in Tubing	9in Long	2	Drawing of part in Appendix C
6	1x1x0.0125in Tubing	20in Long	2	No drawing needed
7	2x1x0.125in C-channel	20in Long	1	Drawing of part in Appendix C
8	Sheet Metal	From Drawing	2	Drawing of part in Appendix C
9	Stock Actuator Bracket	Stock	1	Stock Drawing in Appendix C
10	1.5x1.5x0.125in Tubing	20 in	4	Drawing in Appendix C
11	0.5in bolt (any thread)	3in	2	Stock bolt, get respective nut
12	0.5in bolt (any thread)	5in	8	Stock bolt, get respective nut
13	0.5 in stock actuator bolt	stock	1	No drawing needed

The bill of materials used in the electrical system can be seen summarized in Table 7 below.

Table 7: Electronics Bill of Materials

Component	Count
Arduino Mega 2560	1
BTS7960 Motor Controller	1
PA-17-POT-2000 Linear Actuator	1
ICM20948 IMU	1
Arduino Joysticks	2
CIM Brushed DC Motor	2
Talon SRX Motor Controller	2
12 V – 17 Ah Lead Acid Battery	2

The CIM motor used for the project can be seen below in Figure 30.



Figure 30: CIM motor [10]

The chosen and used motor controllers can be seen below in Figure 31.



Figure 31: Talon SRX Motor Controller [4]

The fuses used in the electrical system can be seen below in Figure 32.

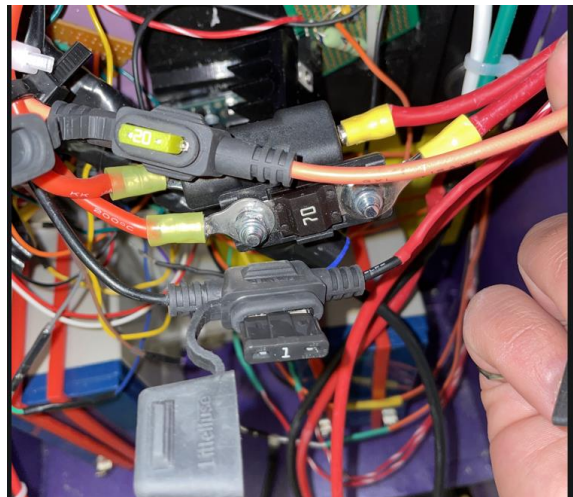


Figure 32: Fuses for all components

The emergency stops implemented can be seen in Figure 33 below.



Figure 33: Emergency Disconnect front and back.

The full assembly of the electrical system can be seen below in Figure 34.

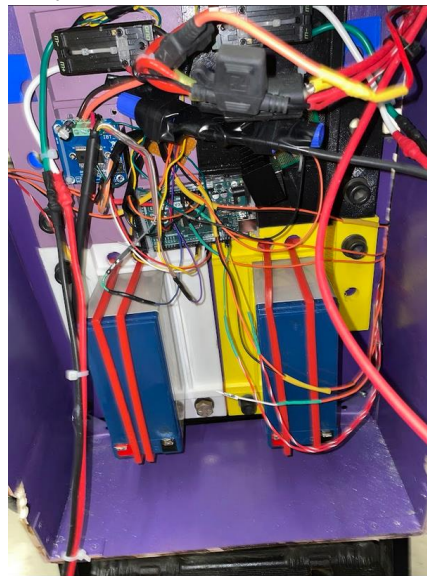


Figure 34: Full CMD electrical assembly.

The initial chassis structure that was designed can be seen below in Figure 35.



Figure 35: Initial Chassis Structure

The FEA done on the initial chassis structure can be seen below in Figure 36.

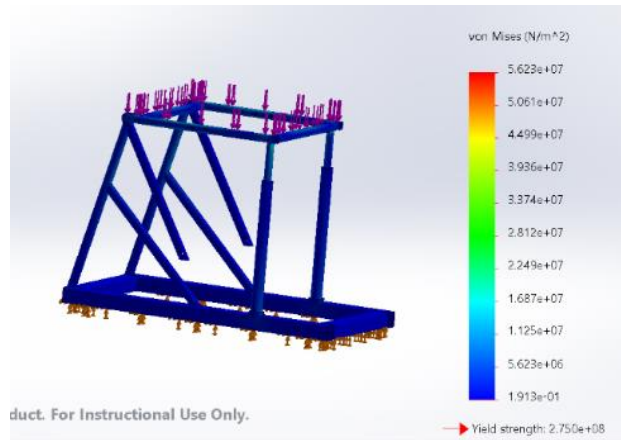


Figure 36: FEA results of stresses.

The complete initial CAD of the project can be seen below in Figure 37.



Figure 37: Complete CAD of the wheelchair.

The new updated design fully assembled can be seen below in Figure 38.

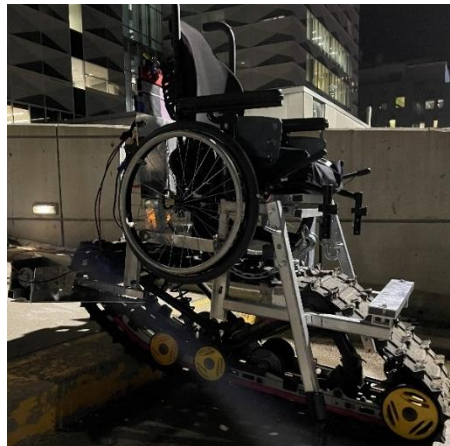
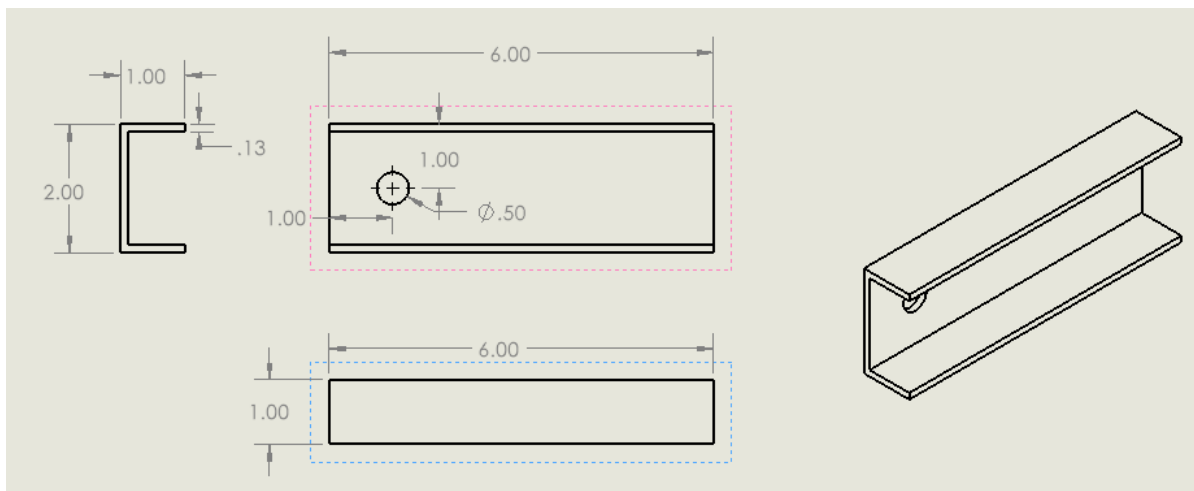
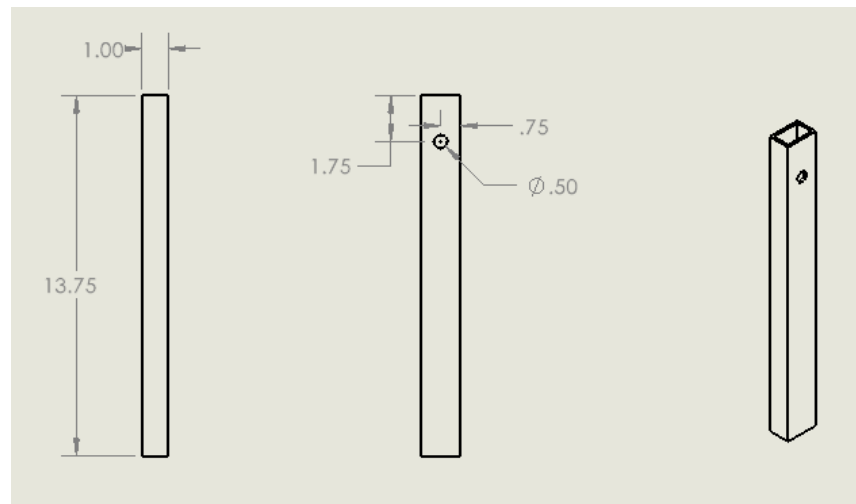


Figure 38: New Design Fully Assembled

Appendix C: As Built Drawings

This appendix will show all the necessary drawings that were used during the manufacturing of the project to assemble the chassis and analyze the specification of the motors.

The drawings for the chassis components that needed to be machined have been referenced by their piece number. This number corresponds to the part in the bill of materials in Appendix B: Bill of Materials and Part References. All the drawings can be seen below in Figure 39, Figure 40, Figure 41, Figure 42, Figure 43, Figure 44, and Figure 45.



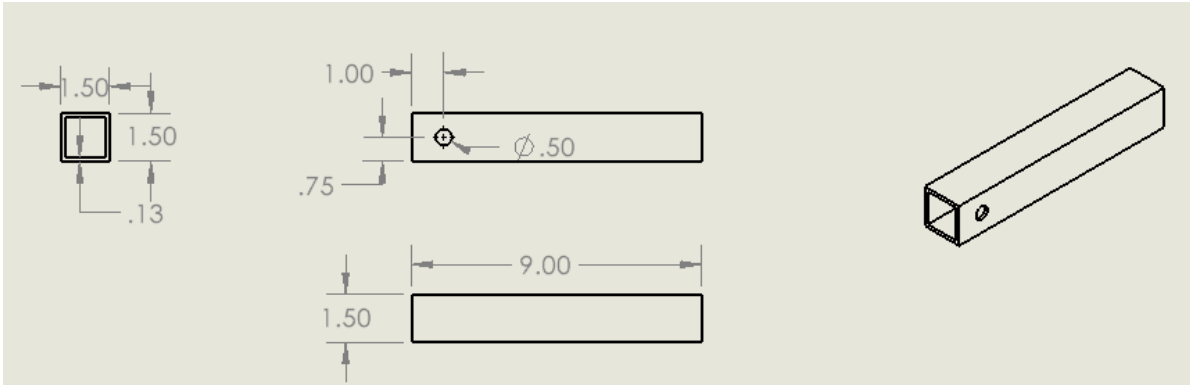


Figure 41: Piece 5 Drawing

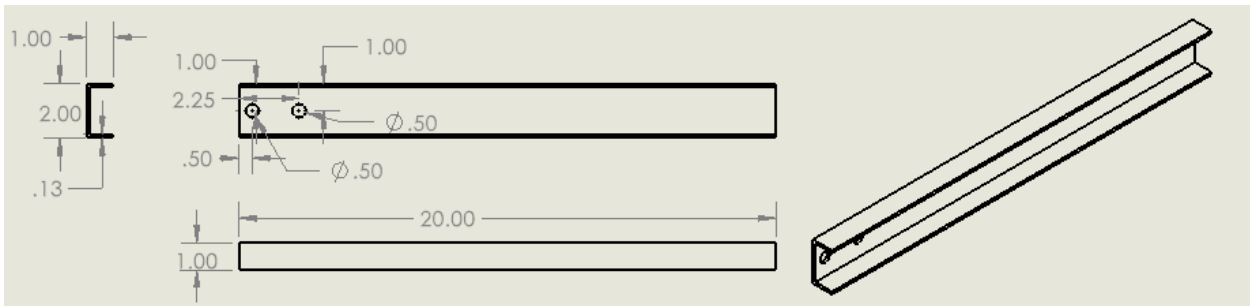


Figure 42: Piece 7 Drawing

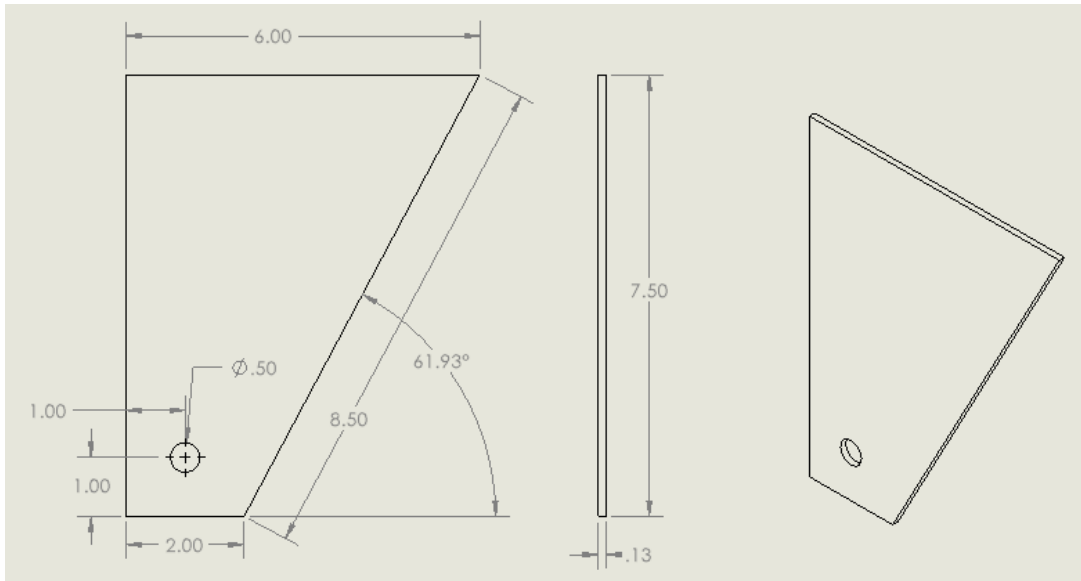


Figure 43: Piece 8 Drawing

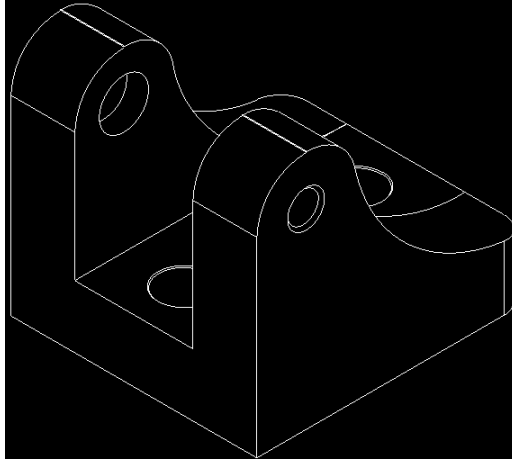


Figure 44: Piece 9 Drawing

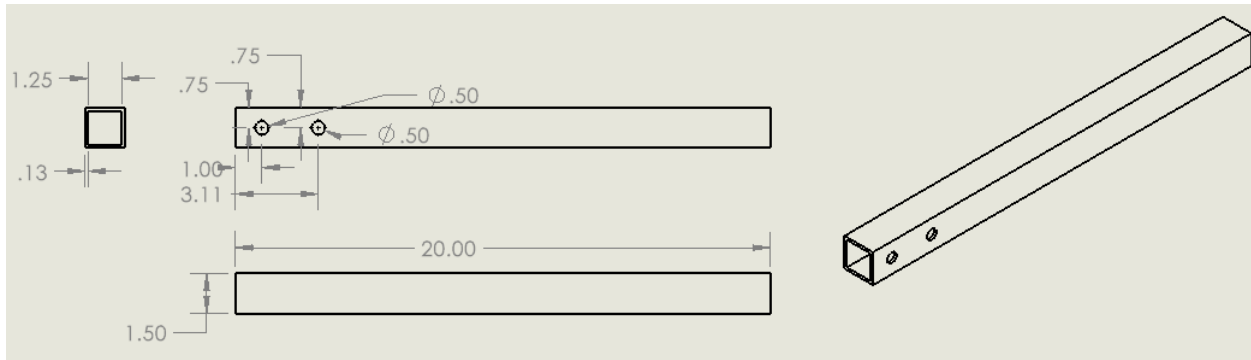


Figure 45: Piece 10 Drawing

The provided stock motor drawing can be seen below in Figure 46 below.

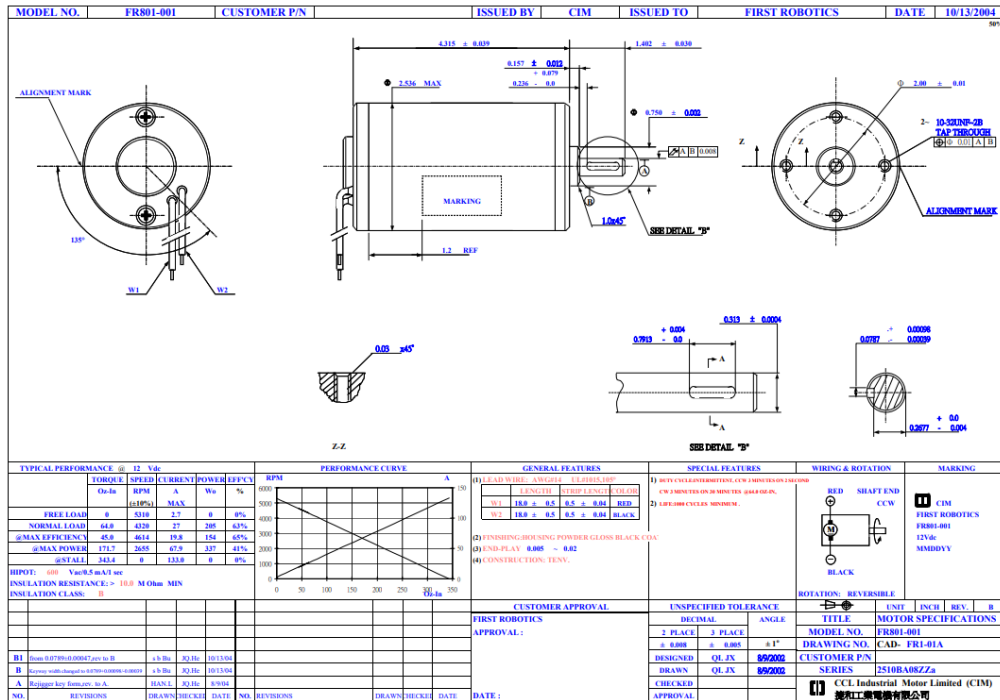


Figure 46: CIM Motor manufacturer specification sheet and component drawing [10]


```

////////// driving ////////////
pinMode(Motor_Joystick_SW_PIN, INPUT_PULLUP); // Set the switch pin as input with
internal pull-up resistor
// Attach the servo objects to pins (must be PWM capable pins on the board)
DriveMotorController1.attach(Drive_PWM_Pin1);
DriveMotorController2.attach(Drive_PWM_Pin2);
// make sure it starts at zero speed
DriveMotorController1.writeMicroseconds(1500); // Range is 1000 - 2000. Motor stops at 1500.
DriveMotorController2.writeMicroseconds(1500);
}

void extendActuator() {
  digitalWrite(Extend_pin, HIGH); // Extend the linear actuator
  digitalWrite(Retract_pin, LOW);
}

void retractActuator() {
  digitalWrite(Retract_pin, HIGH); // Retract the linear actuator
  digitalWrite(Extend_pin, LOW);
}

void stopActuator() {
  digitalWrite(Extend_pin, LOW);
  digitalWrite(Retract_pin, LOW);
}

void resetActuator() {
  int currentPosition = analogRead(Position_pin);

  // Determine the direction to move the actuator to reach the middle position
  if (currentPosition > NEUTRAL_ACTUATOR_POSITION + deadband) { // If the current position
is above the middle
    retractActuator(); // Retract the actuator
    while (analogRead(Position_pin) > NEUTRAL_ACTUATOR_POSITION + deadband) {
      delay(50);
    } // Wait until the actuator reaches the middle
  } else if (currentPosition < NEUTRAL_ACTUATOR_POSITION - deadband) { // If the current
position is below the middle
    extendActuator(); // Extend the actuator
    while (analogRead(Position_pin) < NEUTRAL_ACTUATOR_POSITION - deadband) {
      delay(50);
    } // Wait until the actuator reaches the middle
  }
}

```

```

// Stop the actuator when it reaches the middle position
stopActuator();
}

void loop() {
  Actuator_Joystick_Y_Val = analogRead(Actuator_Joystick_Y_Pin); // Read Y-axis value of the
joystick
  Actuator_Joystick_X_Val = analogRead(Actuator_Joystick_X_Pin); // Read X-axis value of the
joystick
  Actuator_Location = analogRead(Position_pin); // Read position of the linear actuator
  Motor_Joystick_Y_Val = analogRead(Motor_Joystick_Y_PIN); // Read the vertical joystick
value (value between 0 and 1023)

////////// Driving //////////
// speed control
if(Actuator_Joystick_X_Val < 400) {
  speed += 1;
  while(Actuator_Joystick_X_Val < 400) { // wait for joystick to be released again
    delay(10);
  }
  speed = constrain(speed,0,4);
} else if (Actuator_Joystick_X_Val > 600) {
  speed -= 1;
  while(Actuator_Joystick_X_Val > 600) {
    delay (10);
  }
  speed = constrain(speed,0,4);
}

if(Motor_Joystick_Y_Val > 600) {
  DriveMotorController1.writeMicroseconds(1500 - (100 + speed*100));
  DriveMotorController2.writeMicroseconds(1500 + (100 + speed*100));
} else if (Motor_Joystick_Y_Val < 400) {
  DriveMotorController1.writeMicroseconds(1500 + (100 + speed*100));
  DriveMotorController2.writeMicroseconds(1500 - (100 + speed*100));
} else {
  DriveMotorController1.writeMicroseconds(1500);
  DriveMotorController2.writeMicroseconds(1500);
}

if(digitalRead(Motor_Joystick_SW_PIN) == LOW){
  DriveMotorController1.writeMicroseconds(1500);
  DriveMotorController2.writeMicroseconds(1500);
}

```

```

// Wait for the button to be released before continuing
while (digitalRead(Motor_Joystick_SW_PIN) == LOW) {
  delay(10);
}
}

////////// Actuator //////////

// Check if the joystick is pushed up (extend actuator)
if (Actuator_Joystick_Y_Val > 600 && Actuator_Location > 70 + deadband ) {
  retractActuator();
}
// Check if the joystick is pulled down (retract actuator)
else if (Actuator_Joystick_Y_Val < 400 ) {
  extendActuator();
} else {
  stopActuator();
}

// Check if the joystick button is pressed to reset actuator position
if (digitalRead(Actuator_Joystick_SW_PIN) == LOW) {
  resetActuator();
  // Wait for the button to be released before continuing
  while (digitalRead(Actuator_Joystick_SW_PIN) == LOW) {
    delay(10);
  }
}
}
}

```